Spectroscopic and thermodynamic properties in a four-band model for pnictides

L. Benfatto,[1,2,3] E. Cappelluti,[2,3] and C. Castellani[3,2]

[1]*Centro Studi e Ricerche "Enrico Fermi," via Panisperna 89/A, 00184 Rome, Italy*
[2]*SMC Research Center, CNR-INFM, and ISC-CNR, via dei Taurini 19, 00185 Rome, Italy*
[3]*Dipartimento di Fisica, Università "La Sapienza," Piazzale Aldo Moro 2, 00185 Rome, Italy*

In this paper we provide a comprehensive analysis of different properties of pnictides both in the normal and superconducting state, with a particular focus on the optimally doped $Ba_{1-x}K_xFe_2As_2$ system. We show that, by using the band dispersions experimentally measured by angle-resolved photoemission spectroscopy, a four-band Eliashberg model in the intermediate-coupling regime can account for both the measured hierarchy of the gaps and for several spectroscopic and thermodynamic signatures of low-energy renormalization. These include the kinks in the band dispersion and the effective masses determined via specific-heat and superfluid-density measurements. We also show that, although an intermediate-coupling Eliashberg approach is needed to account for the magnitude of the gaps, the temperature behavior of the thermodynamic quantities does not show in this regime a significant deviation with respect to weak-coupling BCS calculations. This can explain the apparent success of two-band BCS fits of experimental data reported often in the literature.

I. INTRODUCTION

The recent discovery of superconductivity in pnictides[1] prompted an intense experimental and theoretical research about the properties of these materials. At the very beginning the analogies between pnictides and cuprate superconductors (e.g., the layered structure and the phase diagram) suggested that a similar route to high-temperature pairing could be at play in these two classes of materials.[2,3] However, a large experimental evidence has been accumulated so far that significant differences between pnictides and cuprates are also important, starting from the very basic fact that pnictides have a multiband structure. According to local density approximation (LDA) calculations, indeed, the band structure of pnictides near the Fermi level is characterized by two holelike bands around the Γ point, and two electron-like bands around the M points of the reduced Brillouin zone.[4–6] A third holelike band at the Γ point could be expected to cross the Fermi level in some materials, but eventually it moves below the Fermi level when the experimental value of the apical As position is used in LDA calculations.[7]

Despite the large theoretical work devoted to address the outcomes of multiband superconductivity, many open issues still remain about a direct comparison between the theoretical predictions and the experiments, or between the outcomes of different experimental probes. A first issue concerns the experimental observation of only two gap values in hole-doped 122 compounds,[8,9] whereas in a multiband BCS approach one would generically expect a different gap in each band, depending on the coupling and on the density of states (DOS) of the several pockets involved in the pairing.[10–12] This is true in particular for hole-doped $Ba_{1-x}K_xFe_2As_2$ (BKFA), where many detailed experimental findings have been accumulating due to the existence of large crystals. Here angle-resolved photoemission spectroscopy (ARPES) has reported quite different DOS in the hole and electron pockets involved in the pairing,[9] so that at the BCS level one could expect to observe three gaps, one for each hole band and one for the (almost degenerate) electron

bands. On the contrary, ARPES experiments have reported only two different gaps: a large one on the inner hole pocket and on the electron ones (with $\Delta/T_c \sim 3.5$), and a small one (with $\Delta/T_c \sim 1.8$) on the outer hole pocket.[8,9]

Besides the non-BCS hierarchy of the gaps, further difficulties arise in the attempt to reconcile ARPES data with several thermodynamic measurements. For instance, photoemission experiments performed by several groups in different pnictide materials have shown that there is a substantial renormalization of the whole band structure with respect to LDA predictions, with a reduction at least of a factor of 2.[9,13–15] At the same time, the estimates of the specific-heat coefficient C_V/T obtained by using the ARPES bandwidth, despite being substantially larger than LDA, are still about a factor two smaller than the values measured in the normal state for 122 compounds.[16–18] This comparison calls for a dichotomy between high-energy and low-energy mass renormalization that must be accounted for by different mechanisms. Recently, a similar distinction between renormalization effects operative at different energy scales has been pointed out also in optical-conductivity measurements in 1111 compounds.[19]

As far as the temperature dependence of the specific heat in the superconducting state is concerned, the comparison with ARPES is again compelling: indeed, despite the large Δ/T_c values reported by ARPES that call for an intermediate/strong coupling pairing mechanism, the temperature profile of the specific heat can be well reproduced by a simple BCS fit.[17,18] A similar result arises from the analysis of superfluid-density measurements,[20–26] where two-gaps BCS fits seem to work quite well once that the experimental Δ/T_c ratios are implemented.

In this paper we provide a systematic analysis of spectral and thermodynamic properties in pnictides with the goal of reconciling the results obtained with the different probes. Our analysis is based on a four-band model where carriers interact with bosonic excitations treated within the Eliashberg approach. As we shall see, the observed hierarchy of the gaps calls for a predominant interband nature of the interac-

tions, making spin fluctuations the most natural candidates for the pairing glue.[27,28] We shall focus in particular on the effects of the exchange of spin fluctuations on several spectroscopic and thermodynamical properties. Since the typical energy scale for spin fluctuations is of the order of 20 meV,[29–32] it cannot be responsible for the overall band narrowing observed by ARPES, that is operative up to a rather high energy. In this context we shall extract input band parameters directly from the high-energy ARPES measurements by assuming that their renormalization with respect to LDA calculations originates from electronic correlations.[33–35] This approach is thus different from what discussed in Ref. 11, when the experimental ARPES determination of the bands for doped BKFA was not yet available. In that case it was shown that, within a BCS approach, the experimental observation of only two gap values could be accounted for by a suitable (moderate) renormalization of the LDA band parameters. Here instead we show that the experimental measurement of the band structure together with the gap values on each band provide in this material a compelling constraint for the microscopic theory. Within this framework we estimate the magnitude of the different interband couplings from a comparison with the measured gaps. We find that the dimensionless couplings vary from $\lambda \simeq 0.2$ to $\lambda \simeq 1.6$, depending on the band. We also calculate the additional mass renormalization due to the exchange of spin fluctuations. These low-energy features are hardly visible in ARPES but they are responsible for the large effective mass of the charge carriers probed by specific-heat measurements that are sensible to excitations near the Fermi level, solving then the apparent contradiction between the different set of measurements. Finally, we analyze the temperature dependence of the specific heat and superfluid density, and we show that at the coupling values relevant for pnictides we do not observe significant deviations from a conventional BCS profile, explaining the apparent success of the BCS fits proposed in the literature.

It is worth pointing out the differences between our approach and previous works on multiband Eliashberg calculations proposed in the literature.[12,36] The tendency of the gaps to assume the same value in strongly nested bands within the Eliashberg theory was already noted in Ref. 12. However, the authors considered there a two-band model, so that it was impossible to reproduce the second smaller gap value measured by ARPES, which is realized in a third, less coupled band. Indeed, a correct approach to pnictides requires using at least a four-band model with an anisotropic interband pairing, as it was pointed out previously within a BCS scheme in Ref. 11. An Eliashberg approach to a four-band model has been explored recently in Ref. 36, where the authors were aimed to reproduce exactly the experimental ratios Δ / T_c in the various bands. An extremely large coupling $\lambda > 4$ was there found for BKFA. Such analysis disregards however the fact that an accurate estimate of T_c within the mean-field-like Eliashberg theory is doubtful in these almost two-dimensional materials, where superconducting fluctuations are expected to be relevant due to the low dimensionality,[37,38] leading to a lowering of the real T_c in comparison with the mean-field estimate. In this situation we prefer to concentrate our analysis on the consistency between the gap values and the density of states. As mentioned above, assuming a typical energy scale $\omega_0 \approx 20$ meV for the characteristic spin-fluctuations, we get $\lambda_i \simeq 0.2–1.6$, much lower than in Ref. 36 (i being here the band index). On the other hand, as we shall show below, these values appear to be perfectly compatible with the thermodynamical properties, whereas stronger couplings would be inappropriate, because the low-energy renormalization of the charge carriers would be too large compared to the experimental outcomes from specific-heat and superfluid-density measurements. Our estimates of the interband coupling $\lambda_i \simeq 0.2–1.6$ in BKFA locate this material in the weak-intermediate-coupling regime. This observation could suggest that analytical expressions *à la* McMillan-Allen-Dynes[39] would be appropriate, as proposed in Ref. 12. This is however not the case in multiband systems where, as we show below, McMillan-Allen-Dynes-like expressions can qualitative fail already above very weak coupling $\lambda \gtrsim 0.2$, so that a numerical solution of the multiband Eliashberg equation is required.

The structure of the paper is the following. In Sec. II, we briefly review the results of a two-band model in order to elucidate the differences between the BCS and Eliashberg approach and the need of a numerical solution even in the weak/intermediate-coupling regime. The reader interested only in the comparison with the experiments can skip this technical discussion, and refer directly to Sec. III, where we introduce the full four-band model, and we show that at intermediate coupling the Eliashberg theory can reproduce the experimentally measured gap values in pnictides. In Sec. IV we show the results for the specific heat and the superfluid density. Finally, in Sec. V we draw some conclusions and we discuss the perspectives of our work.

II. TWO-BAND MODEL

The BCS theory is characterized by a number of universal behaviors (as the T_c vs. λ relation, the $\Delta / T_c = 1.76$ ratio, etc.) which are strictly valid only in the limit where the dimensionless coupling $\lambda \rightarrow 0$. Deviations from these universal results are related to intermediate/strong coupling effects, so that the analysis of such deviations could be employed in principle to estimate the strength of the coupling λ. McMillan-Allen-Dynes-like formulas,[39] based on a controlled expansion in power of λ, could be quite useful in this context because in single-band models they provide analytical expressions to quantify these effects without resorting to a numerical solution of the Eliashberg equations.

In this section we show that in the multiband case with predominant interband interaction the situation is quite different. Indeed, the McMillan-Allen-Dynes-like expansion reproduces the Eliashberg behavior as function of λ only for very weak coupling $\lambda \lesssim 0.2$, whereas for larger couplings a full numerical solution of the Eliashberg equations is required. We demonstrate this result for simplicity within a two-band system, previously addressed in Ref. 12. We thus write the general Eliashberg equations for a purely interband interaction which is taken to be repulsive in the Cooper channel:
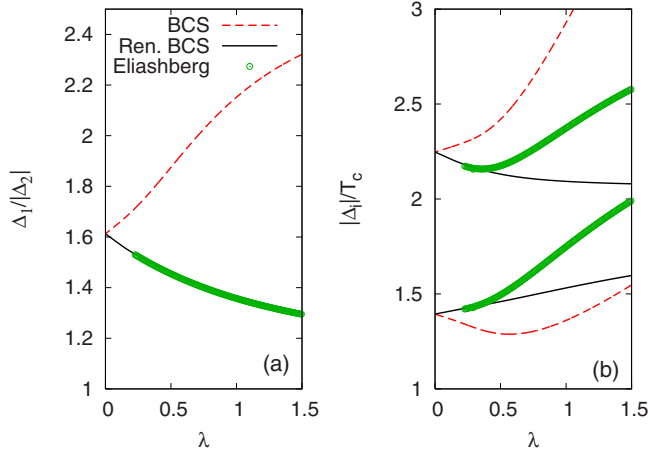
FIG. 1. (Color online) Evolution of the ratio $\Delta_1/|\Delta_2|$ (panel a) and of $|\Delta_i|/T_c$ (panel b) as function of λ calculated by solving numerically the BCS Eqs. (3) and (4), the renormalized BCS Eqs. (5)–(8) and the Eliashberg Eqs. (1) and (2) with $B=2.6$. Notice that while the renormalized BCS model reproduces the behavior of $\Delta_1/|\Delta_2|$ in Eliashberg theory at all coupling values, the same is not true for the $|\Delta_i|/T_c$ values.

$$Z_1(n)\Delta_1(n) = -\lambda_{12}\pi T\sum_m D(n-m)\frac{\Delta_2(m)}{\sqrt{\omega_m^2+\Delta_2^2(m)}}, \quad (1)$$

$$Z_1(n) = 1 + \lambda_{12}\frac{\pi T}{\omega_n}\sum_m D(n-m)\frac{\omega_m}{\sqrt{\omega_m^2+\Delta_2^2(m)}}, \quad (2)$$

together with an equivalent set of equations for Δ_2, Z_2 related through a coupling constant λ_{21}. Here for sake of shortness we denote the dependence on the Matsubara frequency ω_n of the gap function Δ_i and the renormalization function Z_i for the band i as $\Delta_i(n)=\Delta_i(i\omega_n)$ and $Z_i(n)=Z_i(i\omega_n)$. $D(n-m) = D(\omega_n-\omega_m)$ is the boson propagator, which is related to the Eliashberg spectral function $B(\Omega)$ by the relation $D(n-m) = \int 2\Omega d\Omega B(\Omega)/[(\omega_n-\omega_m)^2+\Omega^2]$. The dimensionless coupling constants λ_{12}, λ_{21} can be expressed in term of an unique energy coupling $G>0$ weighted by the appropriate density of states N_i, namely, $\lambda_{12}=GN_2$ and $\lambda_{21}=GN_1$.

Equations (1) and (2) can be solved self-consistently to obtain a numerical exact solution of the Eliashberg equations, assuming, for simplicity, an Einstein boson spectrum $B(\Omega)=(\omega_0/2)\delta(\Omega-\omega_0)$, where ω_0 is the characteristic boson energy. For a repulsive interaction, $G>0$, the gaps in the two bands have opposite signs, so that the order parameter has a $s_\pm$ symmetry. In the rest of the Section we will assume conventionally $\Delta_1>0$ and $\Delta_2<0$. Moreover, to make a direct comparison with Ref. 12, we consider the case where the ratio $B=N_2/N_1$ of the DOS in the two bands is $B=2.6$.

Let us focus first on the gap anisotropy $A \equiv \Delta_1/|\Delta_2|$ at $T=0$ as a function of the average coupling $\lambda \equiv \sqrt{\lambda_{12}\lambda_{21}}$, which was extensively analyzed in Ref. 12. As one can see in Fig. 1(a), $A \to \sqrt{B}$ as $\lambda \to 0$,[12] but within the Eliashberg framework A approaches 1 as λ increases, showing that the gaps get closer to each other. This result is in sharp contrast with the BCS solution that is obtained from Eqs. (1) and (2) by neglecting the equation for the renormalization functions

$[Z_i(n)=1]$, and assuming a BCS factorized square-well model $D(n-m)=\theta(\omega_0-|\omega_n|)\theta(\omega_0-|\omega_m|)$. Within this framework $\Delta_i(n)=\Delta_i\theta(\omega_0-|\omega_n|)$ and one gets the simple equations

$$\Delta_1 = -\lambda_{12}\Delta_2\Pi_2, \quad (3)$$

$$\Delta_2 = -\lambda_{21}\Delta_1\Pi_1, \quad (4)$$

where $\Pi_i=\pi T\Sigma_n\theta(\omega_0-|\omega_n|)/\sqrt{\omega_n^2+\Delta_i^2}$. The behavior of A obtained by the numerical solution of the previous BCS set of equations is also reported in Fig. 1(a): as one can see, the two gap values diverge one from the other as the coupling increases, in contrast to the results of the intermediate-strong coupling Eliashberg solutions of Eqs. (1) and (2).[12]

Since the Eliashberg theory accounts for the effects of the Z renormalization functions, in Ref. 12 it was proposed a simple analytical way to illustrate the difference between BCS and Eliashberg approach by means of a "renormalized BCS model." In this case the square-well model for the gap equations can be completed with a corresponding square-well model for the renormalization spectral functions, $Z_1(n)=1+\lambda_{12}$ and $Z_2(n)=1+\lambda_{21}$ for $|\omega_n|\le\omega_0$ and $Z_1(n)=Z_2(n)=1$ for $|\omega_n|\ge\omega_0$ so that

$$\Delta_1 Z_1 = -\lambda_{12}\Delta_2\Pi_2, \quad (5)$$

$$Z_1 = 1 + \lambda_{12}, \quad (6)$$

$$\Delta_2 Z_2 = -\lambda_{21}\Delta_1\Pi_1, \quad (7)$$

$$Z_2 = 1 + \lambda_{21}. \quad (8)$$

The gap anisotropy obtained from the above set of equations is also shown in Fig. 1(a), compared to the Eliashberg and BCS solutions. Remarkably, one sees that the renormalization effects account very well for the decreases of the gap anisotropy A as the coupling constant increases, giving essentially the same $A(\lambda)$ dependence as the Eliashberg calculations. As it was suggested in Ref. 12, this result can be understood by an analytical approximation of Eqs. (5)–(8) at low coupling. Indeed, at $T=0$ one can use the approximate BCS forms of the Π_i bubbles, $\Pi_i=\sinh^{-1}(\omega_0/|\Delta_i|) \approx \log(2\omega_0/|\Delta_i|)$ to write a self-consistent expression for the ratio A as a function of the dimensionless couplings λ_{12} and λ_{21},

$$\frac{AZ_1}{\lambda_{12}} - \frac{Z_2}{A\lambda_{21}} = \log A. \quad (9)$$

As a consequence, Eq. (9) can be solved perturbatively in powers of the effective coupling $\tilde{\lambda}=\lambda/\sqrt{Z_1 Z_2}$, which takes into account, at a BCS level, the self-energy renormalization,

$$A = \sqrt{\tilde{B}}(1 + c\tilde{\lambda} + d\tilde{\lambda}^2) + \mathcal{O}(\tilde{\lambda}^3), \quad (10)$$

where $\tilde{B}=(Z_2/Z_1)B$. By substituting Eq. (10) into Eq. (9), and recalling that $Z_1\sqrt{\tilde{B}}/\lambda_{12}=Z_2/\sqrt{\tilde{B}}\lambda_{21}=1/\tilde{\lambda}$, we immediately obtain

$$c = \frac{1}{4}\log \widetilde{B}, \quad d = \frac{c + c^2}{2} = \frac{4\log \widetilde{B} + \log^2 \widetilde{B}}{32}. \quad (11)$$

While making an expansion in the coupling constant one must properly expand also $\widetilde{\lambda}$ and $\widetilde{B}$ at the leading order in λ, namely,

$$\widetilde{B} \simeq B(1 + \lambda_{21} - \lambda_{12}), \quad (12)$$

$$\widetilde{\lambda} \simeq \lambda\left(1 - \frac{\lambda_{21} + \lambda_{12}}{2}\right). \quad (13)$$

As a consequence, one finds[14] for the gaps ratio (10)

$$A = \frac{\Delta_1}{|\Delta_2|} = \sqrt{B}\left(1 + \frac{\lambda_-}{2} + \frac{\lambda}{4}\log B\right), \quad (14)$$

where $\lambda_\pm = \lambda_{21} \pm \lambda_{12}$. The BCS case is recovered from the previous equations by setting $Z_1 = Z_2 = 1$, i.e., $\lambda_\pm = 0$. Thus, since $\lambda_- < 0$ when $B > 1$, and the second term is larger than the third one regardless the value of $B > 1$, from Eq. (14) it follows that in the BCS case A increases with increasing λ, while in the presence of renormalization effects A decreases, i.e., the two-gap values approach each other, as confirmed by the numerical solutions at all λ values reported in Fig. 1(a).

From the above considerations and the results of Fig. 1(a) one could then be tempted to conclude, as it was done in Ref. 12, that the McMillan-Allen-Dynes-like Eqs. (5)–(8) capture the basic physics of the Eliashberg solution at all coupling values. However, this is not the case, as we show in Fig. 1(b), where we report explicitly the Δ_i/T_c values in the various approaches. Here we use for simplicity in the BCS and renormalized BCS case the estimate $T_c = 1.13\omega_0 \exp(-1/\lambda)$ and $T_c = 1.13\omega_0 \exp(-1/\widetilde{\lambda})$, respectively, valid at weak coupling by means of the approximate BCS form $\Pi_i = \log(1.13\omega_0/T_c)$ of the bubbles near T_c. As one can see in Fig. 1, in the renormalized BCS case the gap values approach each other by a decrease in the larger Δ_1/T_c value, and a partial increase in the smaller $|\Delta_2|/T_c$ value. This result can be again understood analytically at low coupling by resorting to the above expansion (10) and the T_c expression. We then obtain the leading dependence of Δ_i/T_c on the coupling:

$$\frac{\Delta_1}{T_c} = 1.76\widetilde{B}^{1/4}\left(1 + \widetilde{\lambda}\frac{4\log \widetilde{B} - \log^2 \widetilde{B}}{32}\right)$$

$$= 1.76 B^{1/4}\left(1 + \frac{\lambda_-}{4} + \lambda\frac{4\log B - \log^2 B}{32}\right), \quad (15)$$

$$\frac{|\Delta_2|}{T_c} = 1.76\widetilde{B}^{-1/4}\left(1 - \widetilde{\lambda}\frac{4\log \widetilde{B} + \log^2 \widetilde{B}}{32}\right)$$

$$= 1.76 B^{-1/4}\left(1 - \frac{\lambda_-}{4} - \lambda\frac{4\log B + \log^2 B}{32}\right). \quad (16)$$

Also in this case the terms in $\lambda_- < 0$ are larger than the others, so that one recovers from the above equations that at low coupling Δ_1/T_c decreases and $|\Delta_2|/T_c$ increases as a function
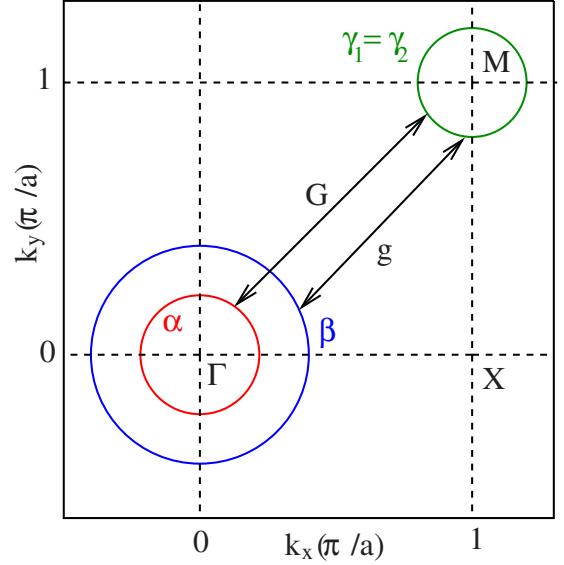

FIG. 2. (Color online) Schematic view of the four-band model we use for pnictides. α and β are the hole bands around the Γ point, $\gamma_1 = \gamma_2$ are the two degenerate electron bands at the M point. The sizes of the pockets are inferred from the experiments in Ba$_{0.6}$K$_{0.4}$Fe$_2$As$_2$ (Ref. 9). The coupling anisotropy, with $G > g$ is suggested by the different nesting properties of electron to the hole bands, as due to their different sizes.

of λ. However, except for a very narrow range of coupling $\lambda \lesssim 0.2 - 0.3$, the numerical Eliashberg solution of Eqs. (1) and (2) is markedly different. Indeed, in the intermediate/strong coupling regime, which is the one relevant for pnictides, both Δ_1/T_c and $|\Delta_2|/T_c$ *increase* with λ in the Eliashberg case. Thus, in the full numerical Eliashberg solution the gaps in the two bands approach each other by means of an increase in the absolute Δ_i/T_c ratio in both the bands, that is the typical signature of strong coupling. We note in passing that while Fig. 1(a) reproduces the findings of Ref. 12, the same is not true for Fig. 1(b). Indeed, the numerical results for Δ_i/T_c in the Eliashberg theory reported in Ref. 12 differ significantly from our findings, even in the low-coupling regime where the above analytical analysis supports completely our numerical calculations.

III. SUPERCONDUCTING PROPERTIES IN A FOUR-BAND MODEL

In the previous section we have shown within a simple two-band model that a full numerical approach is needed to capture the property of Eliashberg equations of removing the DOS anisotropy of the gaps in the presence of interband pairing. Following the same reasoning we focus in this section on a four-band model, to correctly capture the physics of pnictides. In particular, we shall discuss the case of hole-doped Ba$_{0.6}$K$_{0.4}$Fe$_2$As$_2$, using the notation of Refs. 8 and 9, where α (β) is the inner (outer) hole-pocket centered around the Γ point, and γ_1, γ_2 are the two electron-like pockets centered around the M points of the folded Brillouin zone of the FeAs planes (see Fig. 2). The dominant interactions in pnictides are thought to be mainly interband ones, connecting

hole Fermi-sheets with electron Fermi-sheets, through the exchange of spin fluctuations at the antiferromagnetic wavevector $\mathbf{Q}=(\pi,\pi)$.[27,28] The strength of such interband coupling between hole and electron pockets, in these materials, is in addition expected to depend on the relative sizes of the pockets, that naturally affect the nesting condition for the spin fluctuations mediating the pairing. In particular, in BKFA the size of the α and γ_i Fermi surfaces is quite comparable, while the β band has a Fermi surface substantially larger, with a corresponding less degree of nesting. In this situation the interband $\beta-\gamma_i$ coupling g is expected to be significantly smaller than the $\alpha-\gamma_i$ coupling G. In addition, since the two electron pockets have comparable sizes, we assume them for simplicity to be degenerate, and we denote with $N_\gamma=N_{\gamma_1}+N_{\gamma_2}$ the total DOS in the electron pockets. We can write thus the multiband Eliashberg equations in the form:

$$Z_\alpha(n)\Delta_\alpha(n) = -\pi T\sum_m D(n-m)\frac{GN_\gamma\Delta_\gamma(m)}{\sqrt{\omega_m^2+\Delta_\gamma^2(m)}}, \quad (17)$$

$$Z_\beta(n)\Delta_\beta(n) = -\pi T\sum_m D(n-m)\frac{gN_\gamma\Delta_\gamma(m)}{\sqrt{\omega_m^2+\Delta_\gamma^2(m)}}, \quad (18)$$

$$Z_\gamma(n)\Delta_\gamma(n) = -\pi T\sum_m D(n-m)\left[\frac{GN_\alpha\Delta_\alpha(m)}{\sqrt{\omega_m^2+\Delta_\alpha^2(m)}} + \frac{gN_\beta\Delta_\beta(m)}{\sqrt{\omega_m^2+\Delta_\beta^2(m)}}\right], \quad (19)$$

$$Z_\alpha(n) = 1 + \frac{\pi T}{\omega_n}\sum_m D(n-m)\frac{GN_\gamma\omega_m}{\sqrt{\omega_m^2+\Delta_\gamma^2(m)}}, \quad (20)$$

$$Z_\beta(n) = 1 + \frac{\pi T}{\omega_n}\sum_m D(n-m)\frac{gN_\gamma\omega_m}{\sqrt{\omega_m^2+\Delta_\gamma^2(m)}}, \quad (21)$$

$$Z_\gamma(n) = 1 + \frac{\pi T}{\omega_n}\sum_m D(n-m)\left[\frac{GN_\alpha\omega_m}{\sqrt{\omega_m^2+\Delta_\alpha^2(m)}} + \frac{gN_\beta\omega_m}{\sqrt{\omega_m^2+\Delta_\beta^2(m)}}\right]. \quad (22)$$

In the BCS limit, the above equations reduce to the one already discussed in Ref. 11,

$$\Delta_\alpha = -N_\gamma G\Delta_\gamma\Pi_\gamma, \quad (23)$$

$$\Delta_\beta = -N_\gamma g\Delta_\gamma\Pi_\gamma, \quad (24)$$

$$\Delta_\gamma = GN_\alpha\Delta_\alpha\Pi_\alpha + gN_\beta\Delta_\beta\Pi_\beta, \quad (25)$$

and T_c is given by $T_c=1.13\omega_0 e^{-1/\Lambda}$, where, in analogy with the two-band case, we introduce the effective coupling

$$\Lambda = \sqrt{G^2N_\gamma N_\alpha + g^2N_\gamma N_\beta}. \quad (26)$$

It is interesting to notice that in the BCS limit the ratio between the two hole gaps is simply given by the ratio of the

TABLE I. Microscopic band parameters extracted from Ref. 9 by approximating each band with a parabolic form $\varepsilon_i(\mathbf{k})=\varepsilon_i^0-t_i|\mathbf{k}|^2$. $N_i=1/4\pi t_i$ is the DOS and n_i is the number of holes/electrons per unit cell in each band. Note that for the γ_1,γ_2 bands we accounted for the corrections due to the elliptical shape reported in Ref. 9.

	α	β	γ_1,γ_2
ε_i^0 (meV)	28	43	−60
t_i (meV)	54	27.5	160
N_i (eV^{-1})	1.47	2.89	0.50
n_i	0.082	0.24	0.06

corresponding interband couplings, i.e., $\Delta_\alpha(n)/\Delta_\beta(n)=g/G$, *independently* on the relative DOS. The simple experimental observation $\Delta_\alpha/\Delta_\beta\approx 1/2$ would suggest thus, in BCS, $g\approx G/2$. Such constraint does not apply however to a more accurate Eliashberg analysis [Eqs. (17)–(22)], where $\Delta_\alpha(n)/\Delta_\beta(n)=(g/G)Z_\beta(n)/Z_\alpha(n)$, so that, in principle, the ratio of the gaps in the two hole pockets depends both on the couplings and on the DOS of the various bands, requiring thus a more careful analysis.

We employ now Eqs. (17)–(22) to evaluate the microscopic interband couplings G, g from the physical constraints given by the experimental determination of the gap magnitudes on the different bands. We shall apply later this analysis to calculate different superconducting and normal-state properties, as the superfluid density and the specific heat, in order to have an independent check of the reliability of our analysis.

A debated issue in this context is the assess of a proper choice for the underlying normal state electronic bands. Indeed, as we mentioned in the introduction, ARPES measurements in several pnictide families report significant differences in the electronic dispersion compared with LDA calculations, with an apparent renormalization of the whole band structure by a factor of 2.[9,13–15] Most striking, such band narrowing seems to be operative up to very high-energy scales, as it is confirmed also by recent optical sum-rule analysis performed in LaFePO samples.[19] This overall renormalization of the bands with respect to LDA seems thus a general feature of pnictides, probably arising from local Hubbard-like correlations,[33–35] so that it cannot be captured by the coupling of the electrons to low-energy bosonic modes. To take into account this feature, we estimate our input band parameters directly from ARPES experiments that have enough resolution to capture the high-energy mass renormalization. Using the tight-binding fit of the bands reported in Ref. 9, we approximate close to the Fermi level each band as $\varepsilon_i(\mathbf{k})=\varepsilon_i^0-t_i|\mathbf{k}|^2$, where $\mathbf{k}$ is measured with respect to the Γ point for the hole bands and to the M point for the electron bands (see Fig. 2). $N_i=1/4\pi t_i$ is the DOS (per spin) in each band. The band parameters for each band, extracted from Ref. 9, are listed in Table I. To model the spin-mediate interaction, following Ref. 40 and the recent report 32 we use $B(\Omega)=\Omega\omega_0/\pi(\omega_0^2+\Omega^2)$, with the characteristic energy scale $\omega_0=20$ meV estimated from experimental measurements.[29–32]
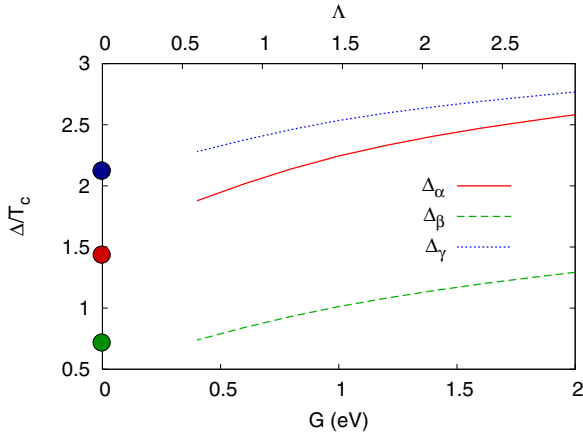
FIG. 3. (Color online) Dependence of the ratios Δ_α/T_c, Δ_β/T_c, and Δ_γ/T_c as functions of the coupling G ($g=G/2$) within the Eliashberg theory. The dots at $G=0$ mark the weak-coupling BCS values.

In approaching a numerical analysis, we should note that, neglecting for the moment the weaker coupling $\gamma-\beta$, the model is equivalent to two-band case discussed in the previous Section, with $B=N_\alpha/N_\gamma \simeq 1.5$, so that at the BCS level the gap values in the two strongly nested bands are different at least by 20%. The presence of a finite scattering $\beta \leftrightarrow \gamma$ makes this scenario even more complex, with the onset of the gap Δ_β, which contributes to increase the magnitude of Δ_γ. In the absence of any particular degeneracy between the α and γ bands, this situation would result, within a weak-coupling BCS framework, in the appearance of three different gaps on the different Fermi sheets, as marked by the dots in Fig. 3. The experimental observation from ARPES of two nearly degenerate gaps on the α and γ bands calls then for further investigation.

In this regard, the strong coupling results from the two-band model, discussed in Ref. 12 and readdressed more specifically in Sec II, shed an interesting light once plugged in a four-band model. Within this context, indeed, the nesting-driven strong coupling interaction between the α and γ bands leads to a merging of the value of the two large gaps Δ_α, Δ_γ in the system. At the same time, the *anisotropy* of the coupling between the two hole pockets and the electron one, guaranteed by the different nesting conditions, allows the system to keep the gap in the β band smaller even within the Eliashberg approach, in agreement with ARPES.

To have a more quantitative insight we plot in Fig. 3 the gap values $\Delta_i=\Delta_i(n=0)$ obtained from the numerical solution at $T=T_c/20$ of Eqs. (17)–(22) as a function of the coupling G, for the indicative case $g=G/2$, which would give the experimental value $\Delta_\beta=0.5\Delta_\alpha$ in the BCS limit $G\to 0$. As we can see, the use of a four-band model is crucial to recover the hierarchy of the gaps: while in the two-band case by increasing λ one is forced to have a single gap value, in the four-band model the anisotropy of the couplings, which follows naturally from the different nesting properties of the various bands, allows for a two-gap result, where two almost degenerate larger gaps are predicted on the electron and on the inner hole pocket, while a smaller gap is found in the outer hole pocket.

TABLE II. Eliashberg parameters obtained by numerical solutions of the Eqs. (17)–(22) with the coupling matrix (27). In the last row we report for comparison also the experimental values of the gaps from Refs. 8 and 9.

	α	β	γ_1, γ_2
Δ_i (meV)	9.48	4.35	−10.48
Z_i (meV)	2.09	1.35	3.67
m_i^*/m_e	9.61	12.28	5.72
$J_{s,i}(0)$ (meV)	4.8	10.7	6.14
$\Delta_i^{\exp}$ (meV)	12 ± 1	6 ± 1	12 ± 1

As mentioned in the introduction, whereas the experimental gaps in the α and γ bands are approximately equal, the ratio $\Delta_\alpha/T_c \approx 3.75$ is quite larger than the BCS value 1.76. Recently, the possibility to reproduce exactly these ratios in BKFA has been investigated in Ref. 36, where it was shown that an extremely large value of the effective coupling $\Lambda \gtrsim 4$ and a small boson energy scale $\omega_0=10$ meV were required. This kind of analysis needs however to be taken with some caution. Indeed, any estimate of T_c in a mean-field-like theory as the Eliashberg one is in general questionable in two-dimensional systems, as pnictides, where the superconducting fluctuations, when properly taken into account, could significantly reduce T_c.[37] For this reason, while the low-temperature gap values estimated within a mean-field-like Eliashberg theory can be quantitatively sound, the estimate of T_c done within the same approach must be taken as an upper limit. Moreover, the values of ω_0 and of the coupling do not influence only the ratios Δ_i/T_c, but they also control in a crucial way other physical quantities, like the mass renormalization and the position of the kink in the band dispersion, that can be accessed experimentally. For these reasons we investigate here the following approach: we discard the exact determination of T_c and we choose the coupling strength as to reproduce the magnitude of the different gap values. Afterward, we check if by means of the same parameter values we can account for other experimental results related to mass renormalization effect in the spectral and thermodynamic properties.

In Table II we summarize our results for the interband scattering, $G=1.1$ eV, $g=0.32G\simeq0.35$ eV, and $\omega_0=20$ meV, obtained to reproduce the experimental gaps. The multiband matrix of the coupling constants, in the band space $(\alpha, \beta, \gamma_1, \gamma_2)$ reads

$$\hat{\lambda} = \begin{pmatrix} 0 & 0 & 0.55 & 0.55 \\ 0 & 0 & 0.18 & 0.18 \\ 1.62 & 1.01 & 0 & 0 \\ 1.62 & 1.01 & 0 & 0 \end{pmatrix}, \qquad (27)$$

and the effective average coupling defined in Eq. (26) is $\Lambda = 1.5$. We notice that a better agreement with the experimental gap values could be enforced by slightly different DOS than the ones estimated in Ref. 9, or by assuming a nonzero interband coupling, as due to phonons. However, we prefer here to use a minimal set of free parameters to show the
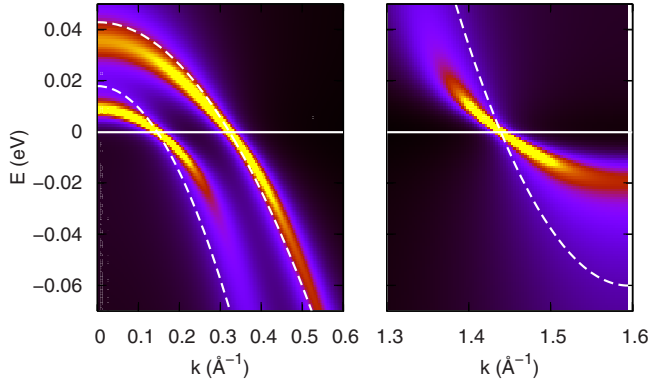
FIG. 4. (Color online) Intensity map of the spectral function in the normal state for the renormalized bands within the Eliashberg theory, as compared to the bare band dispersions, represented by the dashed lines. Note that within a spin-fluctuation model for the bosonic excitation the kink features at $E = -\omega_0$ are considerably smeared out in the spectral functions. Here we added a constant broadening $\eta = 0.002\omega_0$ to account for a small amount of disorder.

overall quantitative agreement between our approach and the experiments. We obtain a critical temperature $T_c = 0.21\omega_0 = 48.7$ K, which overestimates the experimental one $T_c^{exp} = 37$ K by about 10 K. Taking into account that a recent analysis of paraconductivity has shown that this is the typical range of temperature where superconducting fluctuations are active in pnictides,[38] one can expect that the effect of superconducting fluctuations beyond Eliashberg theory will contribute to improve the agreement between the present estimate of T_c and the experimental value.

The coupling of carriers to spin fluctuations reflects on the one-particle spectral properties already above T_c. In particular, the bands in the normal state are expected to display a kink at an energy ω_0, so that for $E < \omega_0$ the Fermi velocity is renormalized with respect to the bare value, with $v_{F,i}^* = v_{F,i}/Z_i$ (or equivalently $m_i^* = Z_i m_{b,i}$), where $Z_i = Z_i(n=0)$ and $m_{b,i}$ is the band mass of the sheet i. In Fig. 4 we show the intensity map of the spectral function for the interacting hole and electron bands, as obtained by the Marsiglio-Schossmann-Carbotte analytical-continuation procedure,[41] along with the bare band dispersions. For the spin-fluctuation model used here, and for the coupling values deduced by the measured gaps, the kinks at ω_0 are significantly smeared out in the spectral function. Unfortunately, the experimental resolution of the data in Ref. 9 is not high enough to resolve the effect of low-energy spin fluctuations from the high-energy renormalization. However, it is interesting to notice that a similar kink has been actually observed in high-resolution ARPES measurements performed by an other group in a BFKA sample with lower doping than the one we are discussing here.[42] In particular, the authors find a kink around approximately 30 meV, and a velocity renormalization in the inner and outer hole pockets of about 1.8 and 1.6. Thus, given the difference in doping and the lack in our approach of a specific momentum dependence of the spin-exchanged fluctuations (that can contribute to slightly increase the effective energy of the kink), our results are in good agreement with these findings.

Below the superconducting transition the position of the kink in the band dispersion is in principle shifted in each

band to an energy given by $\omega_0 + \Delta_j$, where Δ_j is the value of the gap in the bands coupled to the i-th sheet. In particular, in the α, β bands the kink due to spin fluctuations is expected to be recovered at an energy $\omega_0 + \Delta_\gamma \approx 30$ meV, while in the γ_1, γ_2 bands two kinks will appear, at the energies $\omega_0 + \Delta_a \approx 30$ meV and $\omega_0 + \Delta_b \approx 25$ meV. It should be pointed out, however, that, because of the smearing of the spectra in Fig. 4, it would be quite hard to detect the possible splitting in the γ bands due to two different gap values of the α and β bands. At the best of our knowledge, a clear identification below T_c of a continuous shift at higher energy of the kinks observed in the normal state has not been reported yet in pnictides.[43]

Finally, it is worth mentioning that an additional source of discrepancy between the LDA and the experimental bands in pnictides comes from finite-band effects that have been discussed in Ref. 44. Indeed, when the strong particle-hole asymmetry of pnictides is taken into account by considering the finite bandwidth, the spin-mediated interband coupling leads to a shift of the Fermi momenta with respect to LDA, that has been indeed measured in other pnictides by de Haas-van Alphen experiments.[45,46] In the present case we did not compute explicitly these shifts, since they are already included in the band dispersion extracted from the measured ARPES data. Since finite-band effects do not alter qualitatively the self-energy corrections apart from the mentioned energy shift, we solved Eqs. (17)–(22) within the usual infinite-band approximation.

IV. THERMODYNAMIC PROPERTIES

Having determined an appropriate set of band parameters and multiband couplings, we investigate now the effects of the spin-mediated interactions on the thermodynamical properties. Indeed, the signatures of low-energy renormalization are much more easily detectable in thermodynamic measurements of masses enhancement than in photoemission, where a very high resolution is required to resolve the kinks in the band dispersion.

Let us consider as a first insight specific-heat measurements. In the normal state, the coefficient $\gamma_N = C_V/T$ of the linear T term in the specific heat measures the mass enhancement, once compared with the value estimated for noninteracting bands. To clarify the units, we shall refer in the following to the specific heat per formula unit (so that one mole of the materials contains 2 Fe atoms). By expressing the renormalized DOS (per spin) of each band as a function of the renormalized mass m^*, $N_i^* = m_i^*/2\pi$ and, restoring explicitly all the needed dimensional constants, we have that each band contributes to γ_N as

$$\gamma_{N,i} = \frac{2\pi^2 k_B^2}{3} N_i^* N_A a^2 = 1.5 \frac{m_i^*}{m_e} \quad \text{mJ/K}^2 \text{ mol}, \quad (28)$$

where $a = 3.9$ Å is the lattice spacing in BKFA, N_A is the Avogadro number, k_B the Boltzmann constant and m_e the free electron mass. Within LDA one obtains $\gamma_N = 9.26$ mJ/K^2 mol,[6] which is remarkably smaller than the values obtained in doped BKFA, either by direct analysis of
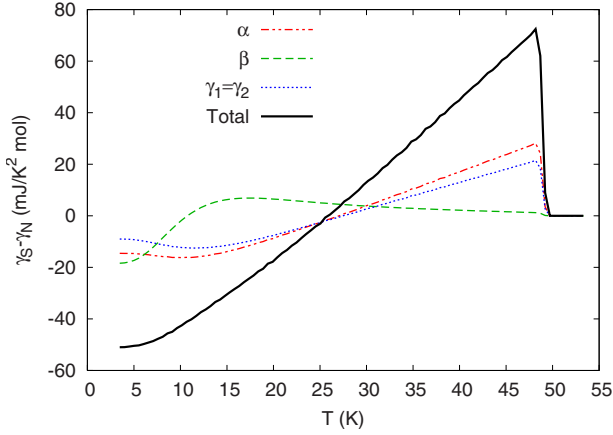
FIG. 5. (Color online) Temperature dependence of the difference between the superconducting and normal-state specific-heat coefficient $\gamma_S - \gamma_N = \Delta C_V / T$ in the various bands, along with the total one.

the normal-state specific heat $\gamma_N \approx 49$ mJ/K^2 mol (Ref. [18]) or by measurements of the upper critical field $\gamma_N \approx 63$ mJ/K^2 mol.[17] By means of the band parameters extracted from ARPES and listed in Table I one estimates $\gamma_N = 25$ mJ/K^2 mol, while with the renormalized masses listed in Table II, that include low-energy renormalization effects on the ARPES bands, we can estimate $\gamma_N = 50$ mJ/K^2 mol, in very good agreement with Ref. [18]. Thus, the additional mass renormalization due to the spin-fluctuations exchange is fundamental to reconcile ARPES and specific-heat measurements. We note that the effective masses obtained until now in the 1111 family by means of de Haas-van Alphen experiments are significantly smaller than the values reported in Table I.[45] This can be attributed to smaller coupling strength, consistently with the smaller T_c values of the 1111 pnictides (see also Ref. [44]). Recently, de Haas van Alphen experiments in BaFe$_2$As$_{1-x}$P$_x$ show a tendency of considerably increase in the mass enhancement for this 122 compound close to the optimal $T_c \simeq 30$ K value.[47] Further de Haas-van Alphen experiments are required to establish the correlation between the mass enhancement and the T_c values that our analysis suggests.

To complete the analysis of the specific heat, we compute numerically the free-energy difference ΔF_i per band between the superconducting and the normal state according to the expression given in Ref. [39], namely,

$$\Delta F_i(T) = -\pi T \sum_n N_i \left[Z_i^S(n) - \frac{Z_i^N(n)|\omega_n|}{\sqrt{\omega_n^2 + \Delta_i^2(n)}} \right]$$
$$\times [\sqrt{\omega_n^2 + \Delta_i^2(n)} - |\omega_n|], \quad (29)$$

where Z_i^S and Z_i^N are the Z-renormalization functions for the i band calculated in the superconducting and in the normal state respectively, and we evaluate the specific-heat difference as $\Delta C_{V,i} = -T \partial^2 \Delta F_i / \partial T^2$. In Fig. 5 we report the temperature dependence of the ratio of the specific heat to temperature for each band, along with the total one $\gamma_S - \gamma_N = \Delta C_V / T = (\Sigma_i \Delta C_{V,i}) / T$. It should be stressed that, given the interband nature of the scattering, the decomposition of the total specific heat ΔC_V in single-band contributions $\Delta C_{V,i}$ is

purely formal since all bands are coupled and the free-energy of one band depends implicitly on the properties of all the other ones. In agreement with what expected in multiband superconductors (see for example Ref. [48] and [49]), at low temperature the increase in γ_S is controlled by the quasiparticle excitations across the smaller gap, i.e., Δ_β in our case, while at higher temperature also quasiparticles excitations in the bands with larger gap are thermally activated. The presence of multiple energy scales for the quasiparticle excitations can lead to the presence of humps in the intermediate temperature range between $T=0$ and T_c, as observed for example in MgB$_2$ compounds.[48,49] In our case, such hump is most evident in the contribution of the band β which is related to the smaller gap. Such hump is not however clearly reflected in the total specific heat since it is partially compensated by the depletion in the other band contributions. The physical origin of such depletions is however questionable since it would give rise to a negative contributions to the specific heat for some band, and it has been argued that it is related to the neglecting of superconducting effects in the boson propagator itself, as a consequence of the electron-boson renormalization.[50] The restoring of a physical positive contribution of the specific heat for all the bands could then make the hump of the β band evident also in the total specific heat. It is worth noting that it is not clear yet if such a hump is visible in the experiments, since it is observed in Ref. [17] but not in Ref. [18], where a temperature profile remarkably similar to the calculations shown in Fig. 5 is reported. Thus, more theoretical and experimental work is required to establish the real temperature profile of the specific heat in pnictides. Finally, we estimate the jump of the specific heat at the transition as $\Delta C_V / T_c = 72.5$ mJ/K^2 mol, so that $\Delta C_V / \gamma T_c = 1.45$. Both are in good agreement with the experimental estimates of $\Delta C_V / T_c = 98$ mJ/K^2 mol and $\Delta C_V / \gamma T_c = 1.5$.[17] As far as $\Delta C_V / \gamma T_c$ is concerned, it must be noticed that even though this estimate is apparently near to the *single-band* BCS value 1.43, actually in the BCS *multiband* case the ratio $\Delta C_V / \gamma T_c$ is no more universal, so that the experimental result cannot be taken as indicative that pnictides are in the weak-coupling regime.

The effect of the multiple gaps is present also in the temperature dependence of the superfluid density n_s, which is experimentally accessible from measurements of the penetration depth λ_L, through the relation $\lambda_L^{-2} = 4\pi e^2 n_s / mc^2$. In two dimensional systems one defines conventionally an energy scale J_s associated to the superfluid density $n_s^{2d} \equiv n_s d$ of each plane such that:

$$J_s = \frac{\hbar^2 n_s^{2d}}{m} = \frac{\hbar^2 c^2}{4\pi e^2} \frac{d}{\lambda_L^2} \Rightarrow J_s \ (\text{K}) = 16.37 \frac{1}{\lambda_L^2 \ [(\mu m)^2]}, \quad (30)$$

where $d=6.6$ Å is the interlayer spacing. Within the Eliashberg approach and in the clean case, J_s can be computed in each band as[39]

$$J_s^i(T) = 2 N_i (v_{F,i} a)^2 \pi k_B T \sum_{n=1}^{\infty} \frac{\Delta_i^2(n)}{Z_i(n)[\omega_n^2 + \Delta_i^2(n)]^{3/2}}. \quad (31)$$

Since we are using a parabolic approximation, at $T=0$ the superfluid density coincides with the carrier density n_i in
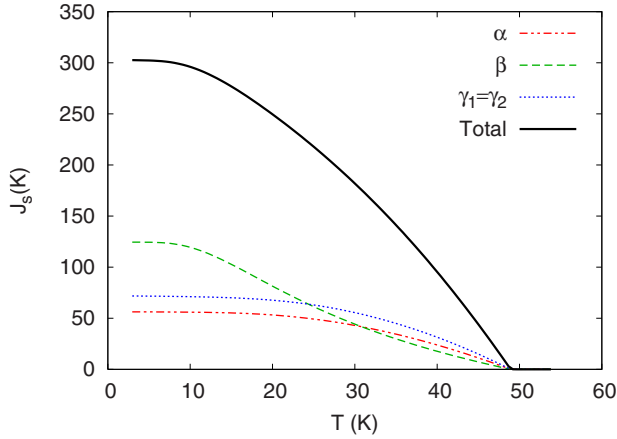
FIG. 6. (Color online) Temperature dependence of the superfluid density in the four bands within Eliashberg theory.

each band, so that Eq. (31) reduces to the standard formula

$$J_s^i(T=0) = \frac{\hbar^2 n_i}{m_i^*} = \frac{2t_i n_i}{Z_i}. \qquad (32)$$

For the band parameters listed in Tables I and II, we can then estimate at $T=0$ $J_s = \Sigma_i J_s^i = 301$ K, while the unrenormalized value (obtained with the ARPES band values but without taking into account the spin-fluctuations induced mass enhancement) would be $J_s \simeq 700$ K.

The temperature dependence of J_s is reported in Fig. 6 and it does not differ considerably from the profile obtained within a simpler multiband BCS approach.[11,51] In all the bands the $J_s^i(T)$ have a flat temperature dependence at low T, typical of exponentially activated quasiparticle excitations across the constant superconducting gaps. In the β band the deviations from the single-band case are more pronounced, due to the low Δ_β/T_c value. This anomaly is reflected also in the total superfluid response, that differs from the standard single-band case. We notice that the α and γ bands have almost the same normalized profile $J_s(T)/J_s(0)$ due to the fact that the gaps have approximately the same value in these two bands. Thus, the curve in Fig. 6 does not differ qualitatively by a BCS two-band calculation, performed assuming that the band with the large gap contributes to 63% of the total superfluid density. This is the reason why two-band BCS fits (implemented with non-BCS values of Δ_i/T_c) work

usually quite well in the comparison with the experimental data.[21,25]

The comparison of our predictions with the experimental data is a quite delicate issue due to the presence of many extrinsic effects which can spoil a robust experimental determination of $J_s(T)$. On one hand, indeed, measurements of microwave surface-impedance have direct access only to $\lambda_L(T) - \lambda_L(0)$ (Refs. 20 and 26) so that the determination of the $\lambda_L^{-2}(T)$ profile usually requires the separate knowledge of $\lambda_L(0)$, even if in some cases one can directly access the normalized penetration depth $\lambda_L^2(0)/\lambda_L^2(T)$.[20] On the other hand, the μSR measurements are also quite delicate because the signal due to the screening supercurrents must be disentangled from the signal due to magnetic domains, an issue particularly delicate in those samples where superconductivity coexists with residual magnetic ordering.[23] A third problem comes from the presence of disorder, which is particularly severe in pnictides due to the $s_\pm$ symmetry of the order parameter, so that interband impurity scattering is pair-breaking and acts in the same way as magnetic impurities in a conventional single-band s-wave superconductor. As a consequence, disorder can lead to a change in the low-temperature superfluid-density profile from the exponential behavior to a power-law behavior in the strong-impurity limit.[52,53] When this is the case, one observes also a strong suppression of $J_s(0)$ with respect to the clean-limit estimate based on Eq. (32).[26] To give a hint about how much spread of the data is present in the literature we summarize some results for hole-doped BKFA in Table III. Note that the exact doping of the samples is not always available, and that for the same nominal doping T_c can be sensibly different, due to the different level of disorder. We also included an estimate of $\lambda_L(0)$ done in Ref. 24 from optical-conductivity data. To make a comparison with our clean-limit estimate (32) of $J_s(0)$ we should then disregard the data characterized by a power-law behavior at low-temperature signature of strong interband impurity scattering, and the data taken for samples with considerably different T_c. The best candidates are then the data from Refs. 21 and 24, which are taken in samples with the same doping level $x=0.4$ and same $T_c = 37–38$ K. These measurement give $J_s(0) = 307–380$ K, which is in very good agreement with our Eliashberg calculations.

Finally, we would like to mention that despite the spread of experimental data, in pnictides the $T=0$ value of the superfluid density is approximately consistent with the value of the Fermi energy, apart the not too large renormalization ef-

TABLE III. Summary of some superfluid-density measurements in BKFA compounds in the literature. The last column indicate the best fit of the temperature dependence at low T, where "Exp" stays for (two-band) exponential fit, and "Pow" stays for power law.

Ref.	x	T_c (K)	$\lambda_L(0)$ (μm)	$J_s(0)$ (K)	Temp. dep.
21	0.4	38	0.231	307	Exp
22	0.45	30	0.569	51	Exp
23	0.5	37	0.298	184	Pow
24	0.4	37	0.208	380	
25		32	0.327	153	Exp
26	0.45	30	0.600	45	Pow

fects discussed here. As it was emphasized already in Ref. 11, this implies generically low values of the superfluid density in pnictides, simply due to the low value of the density of carriers in each band, see Eq. (32). This result must be contrasted with the case of cuprates, where the density of electrons n is large (of order of $n \sim 1-x$, where x is the number of doped holes/electrons), but nonetheless the superfluid density n_s is small, and scales approximately with x, so that $J_s \sim xt$, where t is a typical hopping energy scale.[54] For this reason, the validity of the well-known Uemura plot,[54] i.e., the scaling of T_c with J_s instead of the gap value Δ in underdoped cuprates, does *not* signal any analogy between the two classes of materials. Indeed, in pnictides $T_c \propto J_s \propto \Delta$, with a small J_s simply due to the fact that Fermi energy is small, in cuprates the suppression of J_s with respect to Δ is due to the proximity to the Mott insulator, and the scaling of T_c with J_s can suggest a predominant role of phase fluctuations.[54]

V. CONCLUSIONS

In the present work we propose an intermediate-coupling Eliashberg multiband approach as an appropriate description of low-energy properties of pnictides. As a starting point we use the bands measured by ARPES, where an overall factor two of renormalization of the bands with respect to LDA is observed,[9,13–15] which originates from correlations and cannot be described by the coupling to a low-energy bosonic mode ($\omega_0 \simeq 20$ meV) discussed here within the Eliashberg theory. We focus in particular on BKFA systems, where the multiband structure is accompanied by a pronounced anisotropy of the Fermi-pocket sizes of the hole bands, with an inner hole pocket almost nested to the electron one trough the antiferromagnetic **Q** vector of spin fluctuations. We have shown that the simultaneous observation of two similar gap values in these bands suggests that the predominant pairing is an interband one, as mediated by the spin fluctuations between the set of hole pockets and the set of electron pockets. By comparing the calculations of the gaps with the experimental data we have estimated the value of the interband coupling and we calculated the corresponding low-energy renormalization in several spectral and thermodynamical properties. In particular, we showed that a single set of parameter values can explain in a consistent way the data on the specific heat[17] and on the superfluid density,[21,24] and we can predict the appearance of low-energy kinks in the band dispersions, that are not always resolved in the experiments. Consistently with the mean-field character of Eliashberg theory we overestimate the critical temperature, which in real systems is reduced by superconducting fluctuations,[37] whose relevance has been recently pointed out in the context of paraconductivity measurements.[38] Our analysis questions the possibility of an extreme strong-coupling estimate as the one proposed recently in Ref. 36, because in this case one would find a huge mass renormalization at low energy, that is in disagreement with the experimental measurements of various thermodynamic quantities. Moreover, we have clarified that

one must resort to a full numerical Eliashberg calculation, an issue that has been overlooked in previous studies of multiband models with dominant interband interactions.[12] Indeed we have explicitly shown that in this case the McMillan-Allen-Dynes-like approximate expansion[39] fails already at coupling values $\lambda \gtrsim 0.2-0.3$, well below the ones relevant for pnictides.

While the absolute values of the spectral and thermodynamic properties can be captured only within a four-band Eliashberg theory, we have shown that the temperature dependence of the same quantities do not show significant deviations with respect to a two bands BCS-like behavior, once the renormalized parameters are used. This explains the success of many two-band BCS fits proposed in the literature to reproduce the experimental data. However, these fits must not be taken as indicative of the success of a two-band BCS theory, that would instead completely fails both from the qualitative and quantitative point of view in explaining the physics of pnictides.

While in the present work we focused on BKFA compounds, our results can be extended to other families of pnictides, once that the proper modifications due to the different nesting properties of the various Fermi pockets are taken into account. An interesting example is provided by recent ARPES reports in electron-doped $BaFe_{1.85}Co_{0.15}As_2$ ($T_c = 25.5$ K), where around the Γ point only the β band crosses the Fermi level, and $\Delta_\beta = 6.6$ and $\Delta_\gamma = 5$ meV.[55] In this case, the almost nested bands are the β pocket and the electron pockets γ_i. However, if the bands have the same DOS measured in hole-doped compounds and reported in Table I, the considerable DOS anisotropy between these bands can explain why, even in the presence of the moderately large interband pairing suggested by the Δ_i/T_c values, the gaps still differ by 30%. Our multiband Eliashberg scheme, with nesting-modulated pairing strength, seems a suitable approach to be used to explain the material- and doping-dependent hierarchy of the gaps in these pnictides as well. However, more experimental information on the high-energy band renormalization would be required to get more quantitative results. Indeed, also in $BaFe_{1.85}Co_{0.15}As_2$ one observes the existence of a mass renormalization beyond LDA at energy scales much higher that the one where spin fluctuations are active.[55] A quantitative estimate of these effects would help comparing the overall mass renormalization with recent measurements of the specific-heat in Co-doped BFA,[56] where γ seems to be smaller than what found in K-doped crystals. Indeed, as we suggest in the present work, such a comparison is crucial to elucidate the dichotomy between high-energy and low-energy mass renormalization effects. Thus, further theoretical and experimental investigation in this direction can certainly help understanding the physics of superconducting pnictides.

[1] Y. Kamihara, T. Watanabe, M. Hirano, and H. Hosono, J. Am. Chem. Soc. **130**, 3296 (2008).

[2] M. R. Norman, Physics **1**, 21 (2008).

[3] M. V. Sadovskii, Phys. Usp. **51**, 1201 (2008)

[4] I. I. Mazin, D. J. Singh, M. D. Johannes, and M. H. Du, Phys. Rev. Lett. **101**, 057003 (2008).

[5] D. J. Singh, Phys. Rev. B **78**, 094511 (2008).

[6] F. Ma, Z.-Y. Lu, and T. Xiang, arXiv:0806.3526 (unpublished).

[7] I. I. Mazin, M. D. Johannes, L. Boeri, K. Koepernik, and D. J. Singh, Phys. Rev. B **78**, 085104 (2008).

[8] H. Ding, P. Richard, K. Nakayama, T. Sugawara, T. Arakane, Y. Sekiba, A. Takayama, S. Souma, T. Sato, T. Takahashi, Z. Wang, X. Dai, Z. Fang, G. F. Chen, J. L. Luo, and N. L. Wang, Europhys. Lett. **83**, 47001 (2008).

[9] H. Ding, K. Nakayama, P. Richard, S. Souma, T. Sato, T. Takahashi, M. Neupane, Y.-M. Xu, Z.-H. Pan, A. V. Federov, Z. Wang, X. Dai, Z. Fang, G. F. Chen, J. L. Luo, and N. L. Wang, arXiv:0812.0534 (unpublished).

[10] V. Barzykin and L. P. Gorgov, JETP Lett. **88**, 131 (2008).

[11] L. Benfatto, M. Capone, S. Caprara, C. Castellani, and C. Di Castro, Phys. Rev. B **78**, 140502(R) (2008).

[12] O. V. Dolgov, I. I. Mazin, D. Parker, A. A. Golubov, Phys. Rev. B **79**, 060502(R) (2009).

[13] D. H. Lu, M. Yi, S.-K. Mo, A. S. Erickson, J. Analytis, J.-H. Chu, D. J. Singh, Z. Hussain, T. H. Geballe, I. R. Fisher, and Z.-X. Shen, Nature (London) **455**, 81 (2008).

[14] L. X. Yang, Y. Zhang, H. W. Ou, J. F. Zhao, D. W. Shen, B. Zhou, J. Wei, F. Chen, M. Xu, C. He, Y. Chen, Z. D. Wang, X. F. Wang, T. Wu, G. Wu, X. H. Chen, M. Arita, K. Shimada, M. Taniguchi, Z. Y. Lu, T. Xiang, and D. L. Feng, Phys. Rev. Lett. **102**, 107002 (2009).

[15] M. Yi, D. H. Lu, J. G. Analytis, J.-H. Chu, S.-K. Mo, R.-H. He, R. G. Moore, X. J. Zhou, G. F. Chen, J. L. Luo, N. L. Wang, Z. Hussain, D. J. Singh, I. R. Fisher, and Z.-X. Shen, Phys. Rev. B **80**, 024515 (2009).

[16] N. Ni, S. L. Bud'ko, A. Kreyssig, S. Nandi, G. E. Rustan, A. I. Goldman, S. Gupta, J. D. Corbett, A. Kracher, and P. C. Canfield, Phys. Rev. B **78**, 014507 (2008).

[17] G. Mu, H. Luo, Z. Wang, L. Shan, C. Ren, and H.-Hu Wen, Phys. Rev. B **79**, 174501 (2009).

[18] Ch. Kant, J. Deisenhofer, A. Günther, F. Schrettle, M. Rotter, D. Johrendt, and A. Loidl, arXiv:0910.0389 (unpublished).

[19] M. M. Qazilbash, J. J. Hamlin, R. E. Baumbach, Lijun Zhang, D. J. Singh, M. B. Maple, and D. N. Basov, Nat. Phys. **5**, 647 (2009).

[20] K. Hashimoto, T. Shibauchi, S. Kasahara, K. Ikada, S. Tonegawa, T. Kato, R. Okazaki, C. J. van der Beek, M. Konczykowski, H. Takeya, K. Hirata, T. Terashima, and Y. Matsuda, Phys. Rev. Lett. **102**, 207001 (2009).

[21] M. Hiraishi, R. Kadono, S. Takeshita, M. Miyazaki, A. Koda, H. Okabe, and J. Akimitsu, J. Phys. Soc. Jpn. **78**, 023710 (2009).

[22] A. A. Aczel, E. Baggio-Saitovitch, S. L. Budko, P. C. Canfield, J. P. Carlo, G. F. Chen, P. Dai, T. Goko, W. Z. Hu, G. M. Luke, J. L. Luo, N. Ni, D. R. Sanchez-Candela, F. F. Tafti, N. L. Wang, T. J. Williams, W. Yu, and Y. J. Uemura, Phys. Rev. B **78**, 214503 (2008).

[23] T. Goko, A. A. Aczel, E. Baggio-Saitovitch, S. L. Bud'ko, P. C. Canfield, J. P. Carlo, G. F. Chen, P. Dai, A. C. Hamann, W. Z. Hu, H. Kageyama, G. M. Luke, J. L. Luo, B. Nachumi, N. Ni, D. Reznik, D. R. Sanchez-Candela, A. T. Savici, K. J. Sikes, N.

L. Wang, C. R. Wiebe, T. J. Williams, T. Yamamoto, W. Yu, and Y. J. Uemura, Phys. Rev. B **80**, 024508 (2009).

[24] G. Li, W. Z. Hu, J. Dong, Z. Li, P. Zheng, G. F. Chen, J. L. Luo, and N. L. Wang, Phys. Rev. Lett. **101**, 107004 (2008).

[25] R. Khasanov, D. V. Evtushinsky, A. Amato, H.-H. Klauss, H. Luetkens, Ch. Niedermayer, B. Büchner, G. L. Sun, C. T. Lin, J. T. Park, D. S. Inosov, and V. Hinkov, Phys. Rev. Lett. **102**, 187005 (2009).

[26] C. Martin, R. T. Gordon, M. A. Tanatar, H. Kim, N. Ni, S. L. Bud'ko, P. C. Canfield, H. Luo, H. H. Wen, Z. Wang, A. B. Vorontsov, V. G. Kogan, R. Prozorov, Phys. Rev. B **80**, 020501(R) (2009).

[27] K. Kuroki, S. Onari, R. Arita, H. Usui, Y. Tanaka, H. Kontani, and H. Aoki, Phys. Rev. Lett. **101**, 087004 (2008).

[28] A. V. Chubukov, D. V. Efremov, and I. Eremin, Phys. Rev. B **78**, 134512 (2008).

[29] K. Matan, R. Morinaga, K. Iida, and T. J. Sato, Phys. Rev. B **79**, 054526 (2009).

[30] R. Osborn, S. Rosenkranz, E. A. Goremychkin, and A. D. Christianson, Physica C **469**, 498 (2009).

[31] A. D. Christianson, E. A. Goremychkin, R. Osborn, S. Rosenkranz, M. D. Lumsden, C. D. Malliakas, I. S. Todorov, H. Claus, D. Y. Chung, M. G. Kanatzidis, R. I. Bewley, and T. Guidi, Nature (London) **456**, 930 (2008).

[32] D. S. Inosov, J. T. Park, P. Bourges, D. L. Sun, Y. Sidis, A. Schneidewind, K. Hradil, D. Haug, C. T. Lin, B. Keimer, and V. Hinkov, arXiv:0907.3632 (unpublished).

[33] M. Aichhorn, L. Pourovskii, V. Vildosola, M. Ferrero, O. Parcollet, T. Miyake, A. Georges, and S. Biermann, Phys. Rev. B **80**, 085101 (2009).

[34] S. L. Skornyakov, A. V. Efremov, N. A. Skorikov, M. A. Korotin, Yu. A. Izyumov, V. I. Anisimov, A. V. Kozhevnikov, and D. Vollhardt, Phys. Rev. B **80**, 092501 (2009).

[35] W. L. Yang, A. P. Sorini, C.-C. Chen, B. Moritz, W.-S. Lee, F. Vernay, P. Olalde-Velasco, J. D. Denlinger, B. Delley, J.-H. Chu, J. G. Analytis, I. R. Fisher, Z. A. Ren, J. Yang, W. Lu, Z. X. Zhao, J. van den Brink, Z. Hussain, Z.-X. Shen, and T. P. Devereaux, Phys. Rev. B **80**, 014508 (2009).

[36] G. A. Ummarino, M. Tortello, D. Daghero, and R. S. Gonnelli, Phys. Rev. B **80**, 172503 (2009).

[37] A. Larkin and A. Varlamov, *Theory of fluctuations in superconductors* (Clarendon Press, Oxford, 2005).

[38] L. Fanfarillo, L. Benfatto, S. Caprara, C. Castellani, and M. Grilli, Phys. Rev. B **79**, 172508 (2009).

[39] For a review see J. P. Carbotte, Rev. Mod. Phys. **62**, 1027 (1990) and references therein.

[40] A. J. Millis, Phys. Rev. B **45**, 13047 (1992).

[41] F. Marsiglio, M. Schossmann, and J. P. Carbotte, Phys. Rev. B **37**, 4965 (1988).

[42] D. V. Evtushinsky, D. S. Inosov, V. B. Zabolotnyy, M. S. Viazovska, R. Khasanov, A. Amato, H.-H. Klauss, H. Luetkens, Ch. Niedermayer, G. L. Sun, V. Hinkov, C. T. Lin, A. Varykhalov, A. Koitzsch, M. Knupfer, B. Büchner, A. A. Kordyuk, and S. V. Borisenko, N. J. Phys. **11**, 055069 (2009).

[43] A recent work [L. Wray, D. Qian, D. Hsieh, Y. Xia, L. Li, J. G. Checkelsky, A. Pasupathy, K. K. Gomes, C. V. Parker, A. V. Fedorov, G. F. Chen, J. L. Luo, A. Yazdani, N. P. Ong, N. L. Wang, and M. Z. Hasan, Phys. Rev. B **78**, 184508 (2008)] points out to the presence of dispersion anomalies at significantly larger energies (40 meV and 18 meV for the γ and α

bands, respectively) in the superconducting state of BKFA, that should be ascribed to a different mechanism.

[44] L. Ortenzi, E. Cappelluti, L. Benfatto, and L. Pietronero, Phys. Rev. Lett. **103**, 046404 (2009).

[45] A. I. Coldea, J. D. Fletcher, A. Carrington, J. G. Analytis, A. F. Bangura, J.-H. Chu, A. S. Erickson, I. R. Fisher, N. E. Hussey, and R. D. McDonald, Phys. Rev. Lett. **101**, 216402 (2008).

[46] J. G. Analytis, C. M. J. Andrew, A. I. Coldea, A. McCollam, J.-H. Chu, R. D. McDonald, I. R. Fisher, and A. Carrington, Phys. Rev. Lett. **103**, 076401 (2009).

[47] H. Shishido, A. F. Bangura, A. I. Coldea, S. Tonegawa, K. Hashimoto, S. Kasahara, P. M. C. Rourke, H. Ikeda, T. Terashima, R. Settai, Y. Onuki, D. Vignolles, C. Proust, B. Vignolle, A. McCollam, Y. Matsuda, T. Shibauchi, and A. Carrington, arXiv:0910.3634 (unpublished).

[48] F. Bouquet, Y. Wang, R. A. Fisher, D. G. Hinks, J. D. Jorgensen, A. Junod, and N. E. Philipps, Europhys. Lett. **56**, 856 (2001).

[49] V. G. Kogan, C. Martin, and R. Prozorov, Phys. Rev. B **80**, 014507 (2009).

[50] M. Mansor and J. P. Carbotte, Phys. Rev. B **47**, 9029 (1993); and J. P. Carbotte (private communication).

[51] Y. Bang and H.-Y. Choi, Phys. Rev. B **78**, 134523 (2008).

[52] A. B. Vorontsov, M. G. Vavilov, A. V. Chubukov, Phys. Rev. B **79**, 140507(R) (2009).

[53] Y. Bang, Europhys. Lett. **86**, 47001 (2009).

[54] P. A. Lee, N. Nagaosa, and X.-G. Wen, Rev. Mod. Phys. **78**, 17 (2006).

[55] K. Terashima, Y. Sekiba, J. H. Bowen, K. Nakayama, T. Kawahara, T. Sato, P. Richard, Y.-M. Xu, L. J. Li, G. H. Cao, Z.-A. Xu, H. Ding, and T. Takahashi, Proc. Natl. Acad. Sci. U.S.A. **106**, 7330 (2009).

[56] F. Hardy, T. Wolf, R. A. Fisher, R. Eder, P. Schweiss, P. Adelmann, H. v. Loehneysen, and C. Meingast, arXiv:0910.5006.